Transport in Porous Media (2006) 62: 139–156
DOI 10.1007/s11242-005-0618-8

The Onset of Convection in an Inclined Anisotropic Porous Layer with Oblique Principle Axes

D. A. S. REES[1,⋆], L. STORESLETTEN[2] and A. POSTELNICU[3]
[1]*Department of Mechanical Engineering, University of Bath, Claverton Down, Bath BA2 7AY, U.K.*
[2]*Department of Mathematics, Agder University College, Serviceboks 422, 4604, Kristiansand, Norway*
[3]*Department of Thermo and Fluid Mechanics, Transylvania University of Brasov, Bdul. Eroilor No. 29, Brasov, 2200, Romania*

(Received: 6 November 2003; in final form: 4 January 2005)

Abstract. We consider the onset of convection in an inclined anisotropic porous layer heated from below. To date the principle axes of the permeability and diffusivity tensors have been assumed to be aligned with the coordinate directions. Therefore particular emphasis is laid upon how the basic flow and criteria for the onset of convection are altered by the presence of oblique principle axes. When these axes are not aligned with the coordinate directions and when the ratios of the principle permeabilities or diffusivities are not too large or too small, we find that there is always a smooth transition in the orientation of the most dangerous mode of instability as the inclination increases from the horizontal. In more extreme cases there may be sudden changes in the orientation, Darcy–Rayleigh number and wavenumber.

Key words: free convection, porous layer, inclined layer, anisotropy, oblique axes, instability.

Nomenclature

a, b, c	functions of ξ_1, ξ_2 and γ.
d, e, f	functions of η_1, η_2 and γ.
$\underline{\underline{D}}$	diffusivity tensor.
F, G, F_2, G_2	small perturbations.
$\underline{g}$	gravity vector.
h	height of layer.
$\underline{i}', \underline{j}', \underline{k}'$	unit vectors in the directions of the principle axes.
k	wavenumber.
$\underline{\underline{K}}$	permeability tensor.
p	pressure.
p_0	pressure at $z = 0$.

⋆Author for correspondence: e-mail: d.a.s.rees@bath.ac.uk

P	pressure perturbation.
R	Darcy–Rayleigh number.
t	time.
T	temperature.
T_0	mean temperature.
u, v, w	fluid seepage velocities in the x-, y- and z-directions.
$\underline{u}$	fluid seepage velocity vector.
U, V, W	velocity perturbations in the x-, y- and z-directions.
x	Cartesian coordinate up the inclined layer.
y	horizontal Cartesian coordinate across the layer.
z	Cartesian coordinate normal to the layer.

Greek symbols

α	layer inclination.
β	coefficient of cubical expansion.
γ	orientation of the K_1 principle axis.
ΔT	temperature drop across the layer.
η_1, η_2	diffusivity ratios.
Θ	temperature perturbation.
λ	complex exponential growth rate.
μ	viscosity.
ξ_1, ξ_2	permeability ratios.
ρ_0	reference density.
σ	heat capacity ratio.
ϕ	orientation of roll.
χ	direction of the basic flow.

Superscripts and subscripts

$'$	differentiation with respect to z.
i	Imaginary part.
r	real part.
s	steady basic flow.
1, 2, 3	x, y and z components of the permeability and diffusivity tensors, respectively.

1. Introduction

Convective flow in inclined porous layers heated from below is of interest in many applications. This general problem was first investigated experimentally and theoretically about 30 years ago by several authors including Bories and Monferran (1972), Bories *et al.* (1972), Bories and Combarnous (1973) and Weber (1974). Recently Rees and Bassom (2000) presented a detailed study of the two-dimensional Darcy–Bénard convection in a porous layer at arbitrary inclinations α from the horizontal. A full numerical solution of the linearised disturbance equations was given and detailed graphical results presented. A careful study showed that 31.49° is the maximum inclination angle at which transverse modes can become unstable.

To date, only a few papers deal with the combined effect of anisotropy and layer inclination. The first work to investigate this generic problem

was undertaken by Trew and McKibbin (1994), who considered the onset of convection in a porous layer consisting of two sublayers with different properties. Storesletten and Tveitereid (1999) examined the onset of Darcy–Bénard convection with respect to three-dimensional disturbances in an inclined layer with anisotropic permeability. It turned out that anisotropy in the permeability (but with transverse isotropy) had an essential influence on the identity of the most unstable mode. Depending on the anistropy ratio and tilt angle convection rolls were formed either with axes parallel to the basic flow or with axes perpendicular to it.

There are three further papers which analyse the effect of anisotropy on convection in inclined porous layers: Postelnicu and Rees (2001), Rees and Postelnicu (2001) and Rees and Storesletten (2002). The first is an analytical study which examines the effect of anisotropy in both permeability and diffusivity when the layer is inclined at a small angle from the horizontal. The second is a detailed and extensive numerical study of the effects of anisotropy on layers at arbitrary inclinations. In these papers the authors allowed all three principle permeabilities and diffusivities to have arbitrary values. Both the critical Darcy–Rayleigh number and wavenumber are calculated as α is increased, as well as the angle which the most unstable roll makes with the direction of the basic flow. In this more general scenario there is not always an abrupt transition between the longitudinal and transverse rolls as α increases, but there is sometimes a smooth transition between these limiting states. Rees and Storesletten (2002) consider the combined effect of suction and transverse anisotropy on the instability of the uniform thickness boundary layer which is formed on an inclined heated surface in a porous medium.

In all the above-quoted studies the principle axes are such that one is perpendicular to the bounding surfaces, while one of the remaining two is aligned in the direction of the flow. In the present paper we consider the more general case where the latter restriction is not maintained. Thus we assume that neither of the two principle axes which are parallel to the bounding surfaces is in the direction that the flow takes when the layer is isotropic.

2. Formulation and Governing Equations

We consider the onset of convection in an inclined porous layer of infinite lateral extent. The layer is saturated by a homogeneous fluid and bounded above and below by two impermeable and perfectly heat-conducting plates held at the constant temperatures, $T_0 - (1/2)\Delta T$ and $T_0 + (1/2)\Delta T$, where $\Delta T > 0$. The thickness of the layer is h, the tilt angle α, and the x-, y- and z-axes are placed as shown in Figure 1. The y-axis is horizontal, and the z-axis is perpendicular to the bounding surfaces.

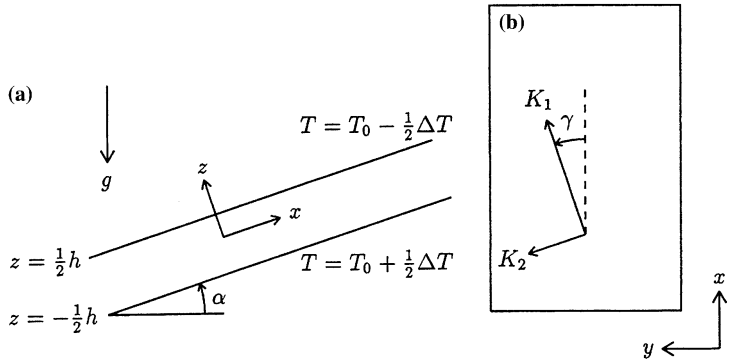

Figure 1. Definition sketch of the inclined layer showing the inclination angle, α, and the orientation of γ, the direction of the K_1 principle axis, relative to the x-direction. (a) side view; (b) plan view.

We assume that the Boussinesq approximation holds, and that no other extension to Darcy's law is present except for anisotropy in the permeability and diffusivity. Therefore the flow and heat transfer are governed by the equations

$$\nabla.\underline{u} = 0, \tag{1}$$

$$\mu\underline{u} + \underline{\underline{K}}.(\nabla p + \rho_0\beta(T - T_0)\underline{g}) = 0, \tag{2}$$

$$\sigma\frac{\partial T}{\partial t} + \underline{u}.\nabla T = \nabla.(\underline{\underline{D}}.\nabla T), \tag{3}$$

where the pressure p includes the hydrostatic pressure, and where the permeability and diffusivity tensors are given by

$$\underline{\underline{K}} = K_1\underline{i}'\underline{i}' + K_2\underline{j}'\underline{j}' + K_3\underline{k}'\underline{k}', \qquad \underline{\underline{D}} = D_1\underline{i}'\underline{i}' + D_2\underline{j}'\underline{j}' + D_3\underline{k}'\underline{k}'. \tag{4}$$

Here the unit vectors, $\underline{i}'$, $\underline{j}'$ and $\underline{k}'$, which represent the directions of the principle axes, are given by

$$\underline{i}' = (\cos\ \gamma, \sin\ \gamma, 0), \quad \underline{j}' = (-\sin\ \gamma, \cos\ \gamma, 0), \quad \underline{k}' = (0, 0, 1). \tag{5}$$

It follows that $\underline{k}'$ coincides with the z-axis, while $\underline{i}'$ and $\underline{j}'$ make an angle γ with the x- and y-axes, respectively. Terms in (1)–(3) have their familiar meanings in the porous medium context and these are given in the Nomenclature.

We introduce the parameters,

$$\xi_1 = \frac{K_1}{K_3}, \qquad \xi_2 = \frac{K_2}{K_3}, \qquad \eta_1 = \frac{D_1}{D_3}, \qquad \eta_2 = \frac{D_2}{D_3}, \tag{6}$$

$$a = \xi_1\cos^2\gamma + \xi_2\sin^2\gamma, \quad b = (\xi_1 - \xi_2)\cos\gamma\sin\gamma, \quad c = \xi_1\sin^2\gamma + \xi_2\cos^2\gamma, \tag{7}$$

$$d = \eta_1\cos^2\gamma + \eta_2\sin^2\gamma, \quad e = (\eta_1 - \eta_2)\cos\gamma\sin\gamma, \quad f = \eta_1\sin^2\gamma + \eta_2\cos^2\gamma, \tag{8}$$

and the dimensionless variables,

$$(x^*, y^*, z^*) = \frac{1}{h}(x, y, z), \quad \underline{u}^* = \frac{h}{D_3}\underline{u}, \quad t^* = \frac{D_3}{\sigma h^2}t, \tag{9}$$

$$p^* = \frac{K_3}{D_3 \mu}p, \quad T^* = \frac{T - T_0}{\Delta T}. \tag{10}$$

The governing Equations (1)–(3) become

$$\frac{\partial u}{\partial x} + \frac{\partial v}{\partial y} + \frac{\partial w}{\partial z} = 0, \tag{11}$$

$$u = -a\frac{\partial p}{\partial x} - b\frac{\partial p}{\partial y} + aRT \sin\alpha, \tag{12}$$

$$v = -b\frac{\partial p}{\partial x} - c\frac{\partial p}{\partial y} + bRT \sin\alpha, \tag{13}$$

$$w = -\frac{\partial p}{\partial z} + RT\cos\alpha, \tag{14}$$

$$\frac{\partial T}{\partial t} + \underline{u}.\nabla T = d\frac{\partial^2 T}{\partial x^2} + 2e\frac{\partial^2 T}{\partial x\,\partial y} + f\frac{\partial^2 T}{\partial y^2} + \frac{\partial^2 T}{\partial z^2}, \tag{15}$$

where the asterisk superscript has been omitted for clarity of presentation. The dimensionless parameter R is the Darcy–Rayleigh number given by,

$$R = \frac{\rho_0 g \beta K_3 \Delta T h}{\mu D_3}, \tag{16}$$

which is based on the permeability and diffusivity in the z-direction. Impermeable and heat-conducting boundaries lead to the conditions,

$$w = 0, \qquad T = \tfrac{1}{2} \text{ on } z = -\tfrac{1}{2}, \quad \text{and} \quad w = 0, \quad T = -\tfrac{1}{2} \text{ on } z = \tfrac{1}{2}. \tag{17}$$

There exists a unique steady basic flow, $\underline{u} = (u_s, v_s, 0)$, $T = T_s(z)$ and $p = p_s(z)$ where the net mass flux through cross-sections $x =$ constant and $y =$ constant are zero. This basic steady state is given by

$$u_s = -aRz \sin\alpha, \quad v_s = -bRz \sin\alpha, \tag{18}$$

$$T_s = -z, \quad p_s = -\tfrac{1}{2}Rz^2 \cos\alpha + p_0, \tag{19}$$

where p_0 is the pressure at $z = 0$.

3. Stability Analysis

The linear stability of the steady basic flow may be investigated by setting

$$\underline{u} = (u_s, v_s, 0) + (U, V, W), \qquad p = p_s + P, \qquad T = T_s + \Theta, \tag{20}$$

where U, V, W, P and Θ are small perturbations of the three velocity components, pressure and temperature, respectively. When substituting (20) into Equations (11)–(15) and eliminating U, V and W, the linearised disturbance equations become,

$$a\frac{\partial^2 P}{\partial x^2}+2b\frac{\partial^2 P}{\partial x\,\partial y}+c\frac{\partial^2 P}{\partial y^2}+\frac{\partial^2 P}{\partial z^2} = R\left[\left(a\frac{\partial\Theta}{\partial x}+b\frac{\partial\Theta}{\partial y}\right)\sin\alpha+\frac{\partial\Theta}{\partial z}\cos\alpha\right], \tag{21}$$

$$\frac{\partial\Theta}{\partial t}=d\frac{\partial^2\Theta}{\partial x^2}+2e\frac{\partial^2\Theta}{\partial x\,\partial y}+f\frac{\partial^2\Theta}{\partial y^2}+\frac{\partial^2\Theta}{\partial z^2}+ + Rz\sin\alpha\left(a\frac{\partial\Theta}{\partial x}+b\frac{\partial\Theta}{\partial y}\right)+R\Theta\cos\alpha-\frac{\partial P}{\partial z} \tag{22}$$

subject to

$$\frac{\partial P}{\partial z}=\Theta=0 \quad \text{on } z=\pm\tfrac{1}{2}. \tag{23}$$

We Fourier-decompose the disturbances in the x- and y-directions which reduces the perturbation equations to ordinary differential eigenvalue form. We therefore substitute

$$P=F(z)e^{ik(-x\,\sin\phi+y\,\cos\phi)+\lambda t}, \quad \Theta=G(z)e^{ik(-x\,\sin\phi+y\,\cos\phi)+\lambda t} \tag{24}$$

into Equations (21) and (22) to obtain

$$F''-k^2(a\,\sin^2\phi-b\,\sin 2\phi+c\cos^2\phi)F = R\left[(\cos\alpha)G'+ik\sin\alpha(-a\sin\phi+b\cos\phi)G\right], \tag{25}$$

$$G''+\left[R\cos\alpha-k^2(d\sin^2\phi-e\sin 2\phi+f\cos^2\phi)\right]G = F'+Rik\sin\alpha(a\sin\phi-b\cos\phi)zG+\lambda G, \tag{26}$$

subject to the boundary conditions,

$$F'=G=0 \quad \text{at} \quad z=\pm\tfrac{1}{2}. \tag{27}$$

Here, $k\sin\phi$ and $k\cos\phi$ are wavenumbers, and ϕ represents the orientation of the axis of the vortex disturbance relative to that of the x-direction. The value $\phi=\pm 90^\circ$ represents the two-dimensional case and is termed a transverse roll, while $\phi=0^\circ$ represents the longitudinal roll. Rolls of other orientations are called oblique.

The critical Darcy–Rayleigh number for any particular configuration of porous medium and roll orientation may be found by setting $\partial R/\partial k=0$.

Therefore we need to solve Equations (25) and (26) together with those formed by taking $\partial/\partial k$ of (25) and (26). If we define $F_2 = \partial F/\partial k$ and $G_2 = \partial G/\partial k$, we may derive the equations,

$$\begin{aligned} &F_2'' - k^2(a\sin^2\phi - b\sin 2\phi + c\cos^2\phi)F_2 \\ &\quad = R\left[(\cos\alpha)G_2' + ik\sin\alpha(-a\sin\phi + b\cos\phi)G_2\right] + \\ &\qquad + 2k(a\sin^2\phi - b\sin 2\phi + c\cos^2\phi)F + \\ &\qquad + Rik\sin\alpha(-a\sin\phi + b\cos\phi)G, \end{aligned} \tag{28}$$

$$\begin{aligned} &G_2'' + \left[R\cos\alpha - k^2(d\sin^2\phi - e\sin 2\phi + f\cos^2\phi)\right]G_2 \\ &\quad = Rik\sin\alpha(a\sin\phi - b\cos\phi)zG_2 + F_2' + i\lambda_i G_2 + \\ &\qquad + 2k(d\sin^2\phi - e\sin 2\phi + f\cos^2\phi)G + \\ &\qquad + Rik\sin\alpha(a\sin\phi - b\cos\phi)zG + i\frac{\partial\lambda i}{\partial k}G \end{aligned} \tag{29}$$

subject to

$$F_2' = G_2 = 0 \text{ at } z = \pm\tfrac{1}{2}. \tag{30}$$

We note that, at the onset of convection, the real part of the exponential growth rate is zero, i.e. $\mathrm{Re}(\lambda) = \lambda_r = 0$, and thus $\lambda = i\lambda_i$.

There are four eigenvalues to find, namely R, k, λ_i and $\partial\lambda_i/\partial k$, and therefore we require four normalisation conditions. Given that Equations (25)–(30) are complex, these four conditions are that

$$G' = 1 \quad \text{and} \quad G_2' = 0 \text{ at } z = -\tfrac{1}{2}. \tag{31}$$

Equations (25)–(30) form an ordinary differential eigenvalue problem consisting of eight second order equations. Although the precise details of the discretisation used, the method adopted and the implementation are given in Rees and Postelnicu (2001), it is important to note that the implementation adopted uses a curve-following strategy, and therefore it is possible to follow the neutral curve around turning points.

One feature of the present problem is that the critical Darcy–Rayleigh number, as calculated by the method outlined above, does depend on the orientation, ϕ, of the convective roll. Therefore we also need to minimise R with respect to ϕ, by setting $\partial R/\partial\phi = 0$. In these circumstances Equations (25)–(30) need to be supplemented with those obtained by differentiating (25) and (26) with respect to ϕ. We omit the presentation of the extra equations for the sake of brevity, but mention that the resulting full system now consists of 12 second order equations with two extra eigenvalues, namely ϕ and $\partial\lambda_i/\partial\phi$.

4. Results and Discussion

4.1. THE BASIC FLOW

It is worth examining the basic flow which arises in this anisotropic layer before presenting the results of the stability analysis since anisotropy with oblique axes has not been considered before in connection with inclined layers. Equation (18) gives the velocity components in the x- and y-directions. Therefore we may define χ as the direction which the flow takes according to

$$\tan \chi = \frac{b}{a} = \frac{(\xi_1 - \xi_2) \tan \gamma}{\xi_1 + \xi_2 \tan^2 \gamma}. \tag{32}$$

In the cases considered by Rees and Postelnicu (2001), for which $\gamma = 0$, this condition simply yields $\chi = 0$ and the basic flow is, not surprisingly, in the direction of the x-axis.

In Figure 2 we display how χ varies with both γ and the ratio ξ_2/ξ_1. When $\gamma = 0^\circ$, which corresponds to nonoblique principle axes, or when $\xi_2 = \xi_1$, which corresponds to a horizontally isotropic medium, then $\chi = 0$. In these cases, even when the medium exhibits thermal anisotropy, the basic flow is in the x-direction. When ξ_2/ξ_1 is particularly small, then flow typically occurs preferentially in the $\underline{i}'$ direction, since the flow is inhibited greatly in the $\underline{j}'$ direction. The $\xi_2/\xi_1 = 0.01$ curve demonstrates this very clearly in Figure 2. In fact, when $\gamma = 45^\circ$ and $\xi_2/\xi_1 = 0.01$, then $\chi = 44.4271^\circ$. But as γ gets close

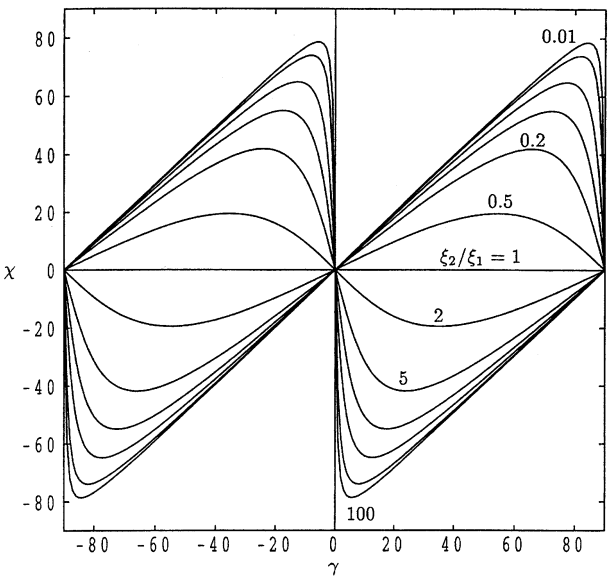

Figure 2. The variation in χ, the direction of the basic flow, as a function of γ for $\xi_2/\xi_1 = 0.01, 0.02, 0.05, 0.1, 0.2, 0.5, 1, 2, 5, 10, 20, 50$ and 100.

to 90° there is a rapid change in χ back towards zero, since buoyancy forces act in the x-direction within the layer.

Such values of χ are also important when interpreting the stability computations below, for when the roll orientation, ϕ, is set equal to χ, then Equations (25)–(30) have real coefficients. Such an angle is always obtained as the most unstable orientation of the rolls in the limit of a vertical layer, and therefore they could be termed 'longitudinal' in view of the fact that the roll axis and the direction of the basic flow are identical. However, we will continue to name as longitudinal those rolls with $\phi = 0°$ and as transverse those with $\phi = 90°$.

4.2. SOME BASIC NEUTRAL STABILITY CURVES

The stability problem we are considering has seven independent parameters, $\xi_1, \xi_2, \eta_1, \eta_2, \phi, \gamma$ and k. An extensive set of results has been obtained but, in the interests of clarity and sufficient brevity we omit those corresponding to anisotropic diffusivity. In all the cases considered here the solutions were of the same nature as those given in Rees and Postelnicu (2001) and therefore we may also minimise R with respect to the wavenumber, k, which reduces the number of parameters to four. We also restrict attention, again for brevity, to cases for which $\xi_1 = 1$; this means that our results are directly comparable with many of those in Rees and Postelnicu (2001). All graphs of the critical Darcy–Rayleigh number feature $R\cos\alpha$ as this value remains finite as $\alpha \to 90°$ for the most dangerous mode.

In Figure 3 we show how the critical value of $R\cos\alpha$ varies with inclination α in the case $\xi_1 = \eta_1 = \eta_2 = 1$ and $\xi_2 = 0.15$. The curves shown correspond to a variety of values of the roll orientation between $-90°$ and 90°, and each frame corresponds to one of four chosen values of γ, the orientation of the K_1 principle axis. Figure 3a shows the stability criterion when $\gamma = 0°$, and therefore it corresponds to Figure 4d of Rees and Postelnicu (2001). In this case the critical value of $R\cos\alpha$ is close to $4\pi^2$ for transverse rolls, for which $\phi = \pm 90°$ when α is small. As α increases, the most unstable roll orientation, which is given by the lowest of the curves, remains the one corresponding to $\phi = \pm 90°$ until the turning point is reached at $\alpha \simeq 31.6°$. At this point the most unstable mode jumps to $\phi \simeq 30°$, and this value decreases smoothly as α increases, and eventually it reaches $\phi = 0$ at $\alpha \simeq 33.1°$. Thereafter the most unstable mode is the longitudinal roll. The quantitative depiction of this transition may be found in Figure 6 of Rees and Postelnicu (2001).

When ξ_2 takes larger values (but still less than unity), then there is a smooth variation in ϕ from 90° to 0°, although this takes place over quite a small range of values of α. For such values of ξ_2 the difference between

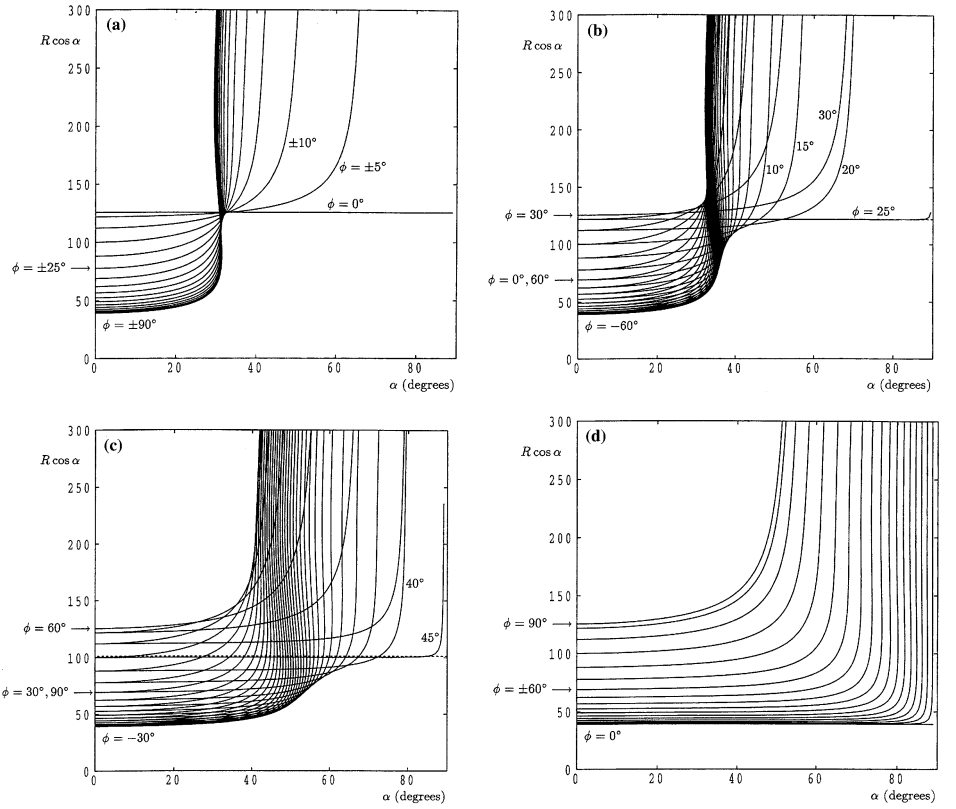

Figure 3. The variation in the critical values of $R\cos\alpha$ as a function of α for a thermally isotropic medium with $\xi_1 = 1$ and $\xi_2 = 0.15$. The different curves correspond to values of ϕ varying in steps of $5°$ from $-90°$ to $90°$. (a) $\gamma = 0°$; (b) $\gamma = 30°$; (c) $\gamma = 60°$; (d) $\gamma = 90°$. The direction of the basic flow in each case is given by: (a) $\chi = 0°$; (b) $\chi = 25.0504°$; (c) $\chi = 45.4361°$; (d) $\chi = 0°$; these values are given by dashed lines in cases (b) and (c).

the small-α and large-α values of $R\cos\alpha$ reduces. We note that all these qualitative effects also occur when (i) $\xi_2 < \xi_1$ for other values of ξ_1 with $\eta_1 = \eta_2 = 1$, and (ii) $\eta_2 > \eta_1$ for general values of η_1 with $\xi_1 = \xi_2 = 1$ although the quantitative details are different.

The identity of the most unstable mode when α is small may be understood by appealing to the fact that the flow is inhibited in the y-direction because $\xi_2 = 0.15$. Therefore fluid motion takes place preferentially in the x- and z-directions. When the inclination of the layer is sufficiently strong the natural tendency for buoyancy forces to dictate the roll orientation means that we recover the longitudinal roll.

Figures 3b–d show how the situation changes as γ takes the respective values $30°$, $60°$ and $90°$. When $\gamma = 30°$ the most unstable mode when $\alpha = 0$

corresponds to $\phi = -60^\circ$ since this direction is again perpendicular to the direction of the K_1 principle axis. As α increases there is a very clear variation in the minimising value of ϕ, and this variation is slower than is the case for $\gamma = 0^\circ$. When α is close to 90°, i.e. the layer is nearly vertical, then most unstable mode has orientation, $\phi = 25.050389^\circ$, which is the direction of the basic flow given by (32). At $\alpha = 0$ there is symmetry about the direction of the K_1 axis in the sense that the critical values of $R\cos\alpha$ are the same for $\phi = \gamma + \delta$ and $\phi = \gamma - \delta$ for arbitrary values of δ. However, when α is nonzero the symmetry is destroyed, and the curves which comprise each pair diverge from one another; this is why pairs of curves emerge from the $R\cos\alpha$ axis.

For $\gamma = 60^\circ$ we see an even slower variation with α of the minimising value of ϕ. In this case the most unstable orientation when $\alpha = 0$ is $\phi = -30^\circ$, and this varies towards $\phi = 45.43611^\circ$ as α increases towards 90°; again see (32). When $\gamma = 90$ the principle axes of the permeability tensor are aligned once more with the coordinate directions. However, the direction with the smallest permeability is now the x-direction, and therefore the y- and z-directions are preferred. Since this corresponds to longitudinal rolls, we find that this orientation is preferred for all values of α. This situation is similar to cases where $\gamma = 0$ and $\xi_2 > 1$.

4.3. THE EFFECT OF VARYING γ ON STABILITY CRITERIA

The graphs shown in Figure 3 are quite typical in shape for any set of parameter values. There will always be one roll direction, as given by (32), where $R\cos\alpha$ remains finite as $\alpha \to 90^\circ$. All other roll orientations find the neutral curve rising sharply and each has a maximum value of α beyond which the curve does not exist. Therefore it is safe to solve Equations (25)–(30), supplemented by those obtained by differentiating (25) and (26) with respect to ϕ, as described earlier, in order to minimise $R\cos\alpha$ with respect to ϕ. Representative results of this process are shown in Figures 4–7.

Figures 4a, b show the minimum value of $R\cos\alpha$ with respect to both k and ϕ for a range of values of γ for a thermally isotropic layer with $\xi_1 = 1$ and ξ_2 equal to 0.15 and 0.4, respectively, while Figure 4c corresponds to the mechanically isotropic case with $\eta_1 = 1$ and $\eta_2 = 20$. In all three cases the lowest line corresponds to $\gamma = 90^\circ$, the critical value of $R\cos\alpha$ is $4\pi^2$ and the mode is the longitudinal roll. For other values of γ the critical value of $R\cos\alpha$ increases monotonically, although the degree of rise when $\xi_2 = 0.4$ is less than that for the more extremely anisotropic case $\xi_2 = 0.15$. This trend continues as ξ_2 decreases towards zero and increases towards 1. In the case when $\xi_2 = 1$, then solutions are clearly independent of γ and

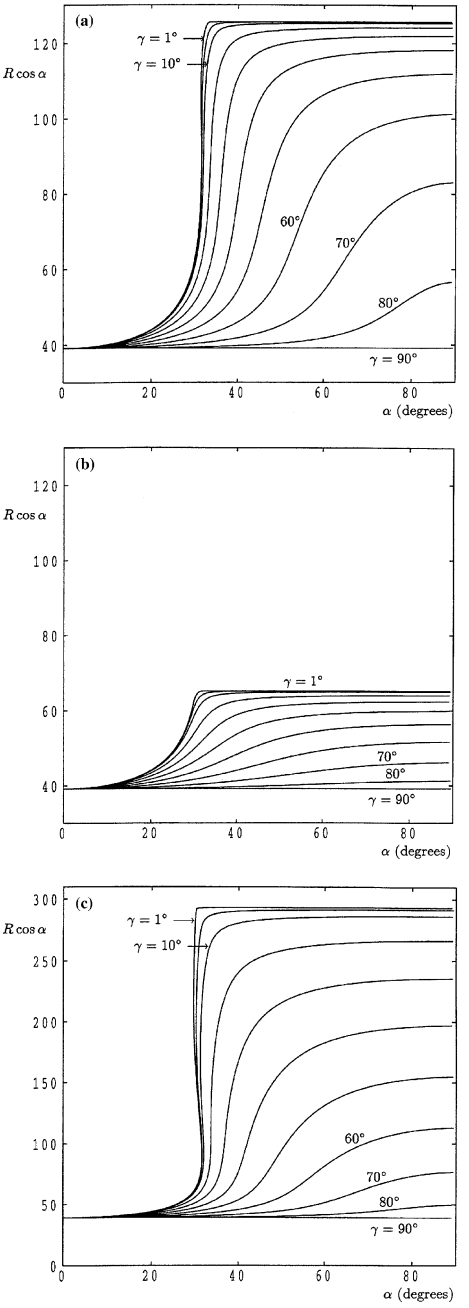

Figure 4. The variation in the critical value of $R\cos\alpha$ as a function of α. These values have been minimised with respect to both k and ϕ. All the parameters ξ_1, ξ_2, η_1 and η_2 are equal to 1 except for (a) $\xi_2 = 0.15$, (b) $\xi_2 = 0.4$ and (c) $\eta_2 = 20$. The different curves correspond to the following values of γ: $1°, 5°, 10°, 20°, 30°, 40°, 50°, 60°, 70°, 80°$ and $90°$.

the common preferred mode is the longitudinal roll whose critical value of $R\cos\alpha$ is $4\pi^2$.

At relatively small values of ξ_2 there are some values of γ where the computed values of $R\cos\alpha$ is no longer a single-valued function of α; this is the same phenomenon as was described above in relation to Figure 3a. Thus the critical value of $R\cos\alpha$ jumps from the turning point to the value directly above it on the upper branch of the curve. This phenomenon persists for smaller values of ξ_2 and exists for a increasingly large range of values of γ as ξ_2 decreases towards zero.

From Figure 4c we see that a large value of η_2 has a qualitatively similar effect to having a value of ξ_2 that is close to zero. The value of η_2 chosen represents a rather extreme case where thermal conduction in the y-direction is 20 times greater than in the other two direction. When γ takes values which are close to zero, then we also have a critical Rayleigh number which increases smoothly as α increases, but which then jumps to a much higher value before resuming a smooth increase.

The corresponding critical values of ϕ are depicted in Figures 5a–c. In all cases the curve corresponding to $\gamma = 1^\circ$ shows that the preferred mode is either very close to the direction of the transverse roll (for small values of α) or close to that of the longitudinal roll (when α is close to 90°). There is a narrow region where the value of ϕ undergoes a very rapid change. As γ increases the width of the transitional region also increases. Although the curves as shown in Figures 5a and 5b are essentially independent of ξ_2 when α is small, they become highly dependent on ξ_2 when α gets close to 90°. There is again less variation in the ultimate roll orientation in the vertical limit when ξ_2 gets closer to 1. In these cases the ultimate roll direction is given by $\phi = \chi$, as given by (32). The same is true for the case shown in Figure 5c, although we now have $\chi = 0^\circ$.

Figures 6a–c show the respective critical wavenumbers. There is, once more, more variation in these values when the porous medium deviates more from isotropy. At low inclinations the critical wavenumber is close to π.

4.4. THE EFFECT OF VARYING ξ_2 ON STABILITY CRITERIA

Finally, we display in Figure 7a–c the critical values of $R\cos\alpha, \phi$ and k/π for $\gamma = 45^\circ$ and for a range of values of ξ_2. All these critical values are independent of ξ_2 when $\xi_2 < \xi_1$ and when $\alpha = 0$ since the flow takes place in the plane defined by $\underline{i}'$ and $\underline{k}'$. At this value of γ the neutral curve for $R\cos\alpha$ has multiple values only when ξ_2 is less than a value between 0.05 and 0.1. When the layer is strongly anisotropic the preferred roll orientation is less strongly affected by the inclination of the layer as α increases until a sudden change occurs at $\alpha = 41.07^\circ$ at which point the preferred

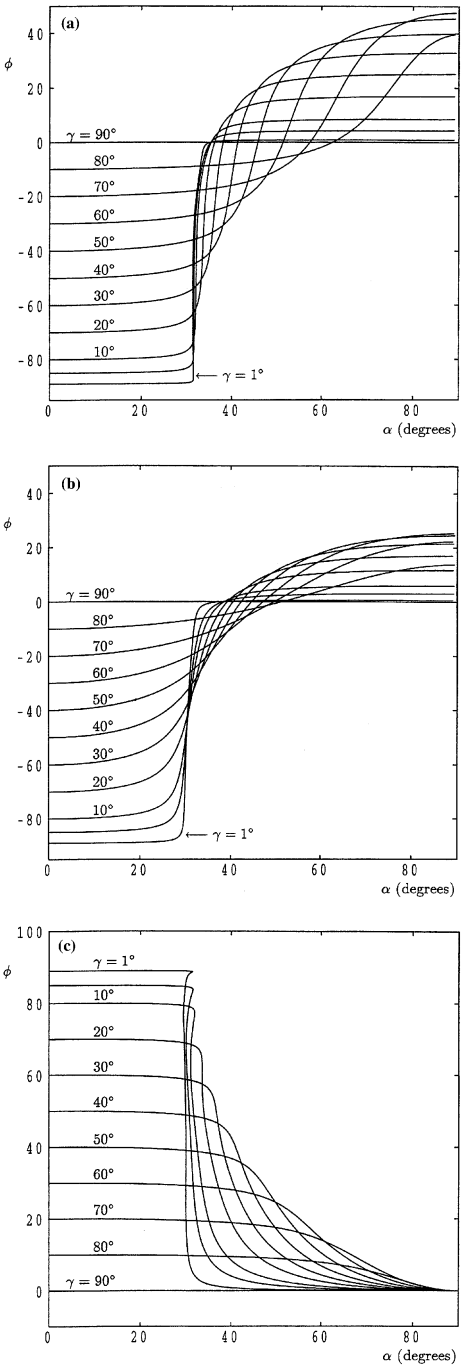

Figure 5. The variation in the critical value of ϕ as a function of α. All values of ξ_1, ξ_2, η_1 and η_2 are equal to 1 except for (a) $\xi_2 = 0.15$, (b) $\xi_2 = 0.4$ and (c) $\eta_2 = 20$. These curves correspond to those given in Figure 4a.

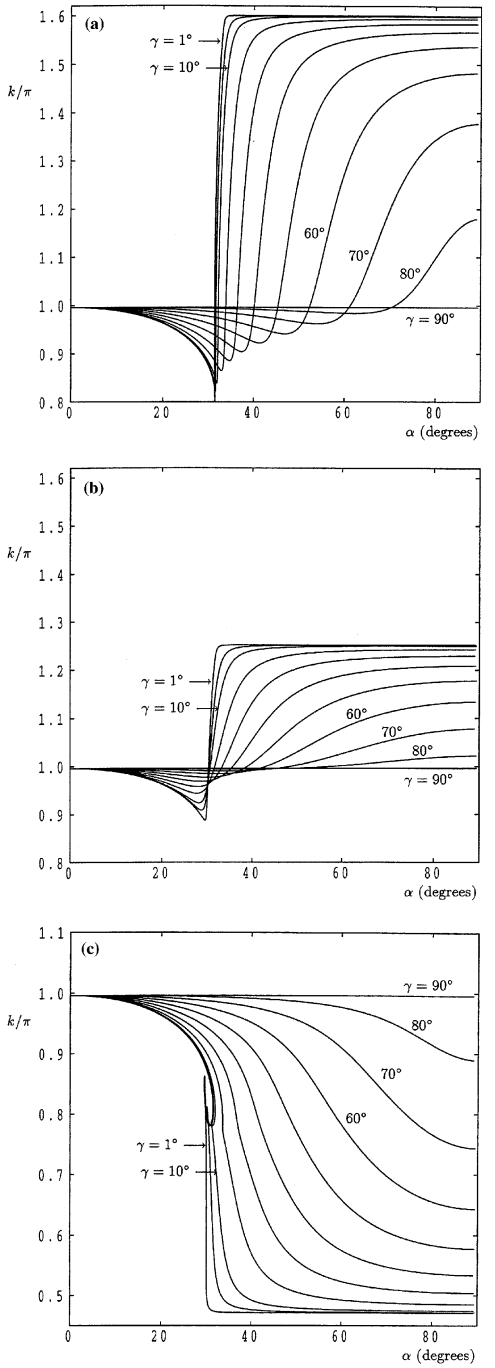

Figure 6. The variation in the critical value of k/π as a function of α. All values of ξ_1, ξ_2, η_1 and η_2 are equal to 1 except for (a) $\xi_2 = 0.15$, (b) $\xi_2 = 0.4$ and (c) $\eta_2 = 20$. These curves correspond to those given in Figure 4a.

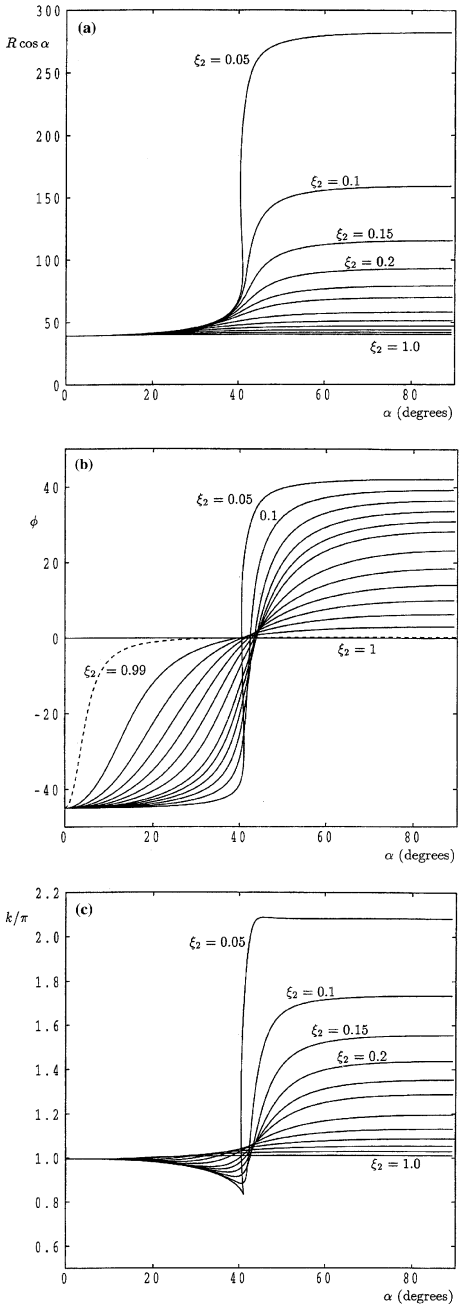

Figure 7. The variation in (a) the critical value of $R\cos\alpha$ as a function of α when $\gamma = 45^\circ$ and the corresponding values of (b) ϕ and (c) k/π for a thermally isotropic medium with $\xi_1 = 1$ and ξ_2 taking the values, 0.05, 0.1, 0.15, 0.2, 0.3, 0.4, 0.5, 0.6 0.7, 0.8, 0.9 and 1.0. The value of R has been minimised with respect to both k and ϕ.

value of ϕ changes from -29.0° to 22.0°. The critical value of $R\cos\alpha$ also jumps from 92.5 to 211.9, and k/π from 0.837 to 1.69. As $\xi_2 \to 1$ the curves corresponding to $R\cos\alpha$ and k/π tend uniformly to a constant value which is independent of α. However, the critical orientation, ϕ, does not converge uniformly since there is always a small region very close to $\alpha = 0$, where ϕ varies rapidly from -45° to close to zero.

5. Conclusions

In this paper we have extended the work of Rees and Postelnicu (2001), on the effects of anisotropy on the onset of convection in an inclined layer, with emphasis on the identity of the preferred roll orientation, to cases where the principle axes of the permeability tensor are rotated about the normal to the layer. Anisotropy with oblique axes has not been considered before in convection within inclined layers. This misalignment causes the basic flow to have a spanwise component in general, and the direction of the flow always satisfies $\chi \leqslant |\gamma|$, with equality only when $\gamma = 0$.

In general we have found that there is usually a gradual variation in the preferred roll direction as the inclination increases. When the degree of anisotropy is sufficiently great, then there exist sudden changes, not only in the preferred orientation of the roll, but also in the critical Darcy–Rayleigh number and wavenumber. Although we have concentrated mainly on cases for which $\xi_2 < 1$ with $\xi_1 = \eta_1 = \eta_2 = 1$, qualitatively similar results also apply when $\eta_2 > 1$ with $\xi_1 = \xi_2 = \eta_1 = 1$, as shown in Figures 4c, 5c and 6c, even though the basic flow is now in the x-direction.

Finally, it is worth commenting on how the above conclusions may be changed when more realistic situations are considered. Many more papers are now appearing which attend to how boundary and form-drag effects affect aspects of flows within porous media. In the present situation both of these effects will change the criterion for the onset of convection, and we think that the critical Rayleigh number is likely to rise compared with corresponding Darcy-flow cases. It is also highly likely that form-drag effects (the Forchheimer terms) will affect quite strongly the preferred orientation of the cells. On the other hand, boundary effects, as modelled by the Brinkman terms and which are usually characterised by a very small Darcy number, are unlikely to change either the critical Rayleigh number or the preferred orientation by a large amount – an example of such a small change in the context of the horizontal Darcy–Bénard problem may be found in Rees (2002) wherein the author shows that the critical Rayleigh number is $4\pi^2(1 + 2\mathrm{D}^{1/2} + \cdots)$ when the Darcy number, D, is small.

A second configuration of interest is when the layer is finite in the spanwise direction. When the layer is isotropic, or if $\gamma = 0$ when the layer

is anisotropic, then typical sidewall boundary conditions (insulating and impermeable) may be satisfied by taking a pair of rolls at orientations $\pm\phi$. This may be done because the governing equations are symmetric about the direction given by the x-axis. Therefore the results of Storesletten and Tveitereid (1999), Postelnicu and Rees (2001) and Rees and Postelnicu (2001) may be applied. However, for more general anisotropies such as are considered in this paper, this symmetry about the x-direction is lost. Therefore the analysis must be reworked by including rectangular planforms explicitly within the stability analysis, and we would expect the onset criterion to change.

References

Bories, S. and Combarnous, M.: 1973, Natural convection in a sloping porous layer, *J. Fluid Mech.* **57**, 63–79.

Bories, S., Combarnous, M. and Jaffrennou, J. Y.: 1972, Observation des différentes formes d'écoulements thermoconvectifs dans une couche poreuse inclinée, *C.R. Acad. Sci. Paris* **A275**, 857–860.

Bories, S. and Monferran, L.: 1972, Condition de stabilité et échange thermique par convection naturelle dans une couche poreuse inclinée de grande extension, *C. R. Acad. Sci. Paris* **B274**, 4–7.

Postelnicu, A. and Rees, D. A. S.: 2001, The onset of convection in an anisotropic porous layer inclined at a small angle from the horizontal, *Int. Com. Heat Mass Transfer* **28**, 641–650.

Rees, D. A. S.: 2002, The onset of Darcy-Brinkman convection in a porous layer: an asymptotic analysis, *Int. J. Heat Mass Transfer* **45**, 2213–2220.

Rees, D. A. S. and Bassom, A. P.: 2000, The onset of Darcy–Bénard convection in an inclined layer heated fom below, *Acta Mechanica* **144**, 103–118.

Rees, D. A. S. and Postelnicu, A.: 2001, The onset of convection in an inclined anisotropic porous layer, *Int. J. Heat Mass Transfer* **44**, 4127–4138.

Rees, D. A. S. and Storesletten, L.: 2002, The linear instability of a thermal boundary layer with suction in an anisotropic porous medium, *Fluid Dyn. Res.* **30**, 155–168.

Storesletten, L. and Tveitereid, M.: 1999, Onset of convection in an inclined porous layer with anisotropic permeability, *Appl. Mech. Engng*. **4**, 575–587.

Trew, M. and McKibbin, R.: 1994, Convection in anisotropic inclined porous layers, *Transport Porous Media* **17**, 271–283.

Weber, J. E.: 1974, Thermal convection in a tilted porous layer, *Int. J. Heat Mass Transfer* **18**, 474–475.